LA-13610-MS

A Natural Analogue for Thermal-Hydrological-Chemical Coupled Processes at the Proposed Nuclear Waste Repository at Yucca Mountain, Nevada

Los Alamos
NATIONAL LABORATORY

Los Alamos National Laboratory is operated by the University of California for the United States Department of Energy under contract W-7405-ENG-36.

An Affirmative Action/Equal Opportunity Employer

LA-13610-MS

Issued: August 1999

A Natural Analogue for Thermal-Hydrological-Chemical Coupled Processes at the Proposed Nuclear Waste Repository at Yucca Mountain, Nevada

Peter C. Lichtner
Gordon Keating
Bill Carey

Los Alamos
NATIONAL LABORATORY
Los Alamos, New Mexico 87545

TABLE OF CONTENTS

ABSTRACT 1

1 INTRODUCTION 2

2 THC COUPLED PROCESSES ASSOCIATED WITH THE PROPOSED YUCCA MOUNTAIN REPOSITORY 3

3 PAIUTE RIDGE INTRUSIVE COMPLEX AS A NATURAL ANALOGUE 4

3.1 Paiute Ridge Geology 4

3.2 Hydrothermal System 11

3.3 Chemical Reactions 17

4 CRITERIA FOR SELECTING AN INTRUSIVE BODY AS A NATURAL ANALOGUE 19

5 CRITIQUE OF MATYSKIELA (1997) 21

6 CONCLUSION 23

7 ACKNOWLEDGEMENTS 23

8 REFERENCES 24

APPENDIX: ANALYSIS OF MATYSKIELA'S (1997) DIFFUSION MODEL 27

A.1 Model Formulation 27

A.1.1 Infinite Length System 29

A.1.2 Finite Length System 30

A.1.2.1 Concentration Boundary Condition 30

A.1.2.2 Zero-Flux Boundary Condition 31

A.2 Variable Surface Area 31

A.3 Fit to Observed Porosity Profile 32

A.4 References 34

LIST OF TABLES

1 Hydrothermal Model Parameters 13

2 Silica Precipitation Modeling Parameters 32

LIST OF FIGURES

1 Geologic map of the Slanted Buttes, Half Pint Range, Nevada. Inset map shows the location of Slanted Buttes. The geologic map indicates the sample locations of tuffs intruded by dikes and sills. 6

2 Cross sections through Paiute Ridge area (A-A′ and B-B′ in Figure 1) showing present day topography and geology, with inferred topography (dashed) at the time of basaltic activity. Legend is the same as in Figure 1. 7

3 Schematic illustration of a possible mineral alteration paragenesis adjacent to a dike intruded into vitric tuff. 9

4 Field observation of a 10 cm opal alteration zone (located behind rock hammer) occurring below a basaltic sill (not visible). 11

5 Schematic diagram of a one-dimensional simulation indicating the initial temperature of the intrusion and tuff country rock. 12

6 Temperature profiles computed by using an equivalent continuum model with the parameters listed in Table 1 with an initial saturation of 0.4. Results are plotted as a function of time, at fixed distances of 1, 10, 25, and 50 m from the intrusion. Shown are intrusive widths of (a) 10 m, (b) 30 m, and (c) 50 m. 14

7 Temperature profiles computed by using an equivalent continuum model, with the parameters listed in Table 1. Initial saturations of 0.4 and 0.6 are used in the calculation. Results are plotted as a function of time, at fixed distances of 1, 10, 25, and 50 m from the intrusion. An intrusive width of 30 m is used in the calculations. 16

8 Liquid saturation profiles computed using an equivalent continuum model with the parameters listed in Table 1. Initial saturations of 0.4 and 0.6 are used in the calculations. Results are plotted as functions of time, at fixed distances of 1, 10, 25, and 50 m from the intrusion. An intrusive width of 30 m is used in the calculations. 16

9 Distributions of (a) temperature, (b) saturation, (c) temperature and saturation profiles at a fixed depth of 150 m, and (d) liquid flow in a two-dimensional flow field surrounding the Papoose Lake intrusion, 100 years after the emplacement of a 1000°C sill. Boundaries include a water table condition along the bottom, 5 mm/yr infiltration along the top, and no-flow sides; see text for a more detailed description of the model domain. The rectangles along the upper right boundary in plots (a) and (b) represent the dimensions of the sill. Note the change of horizontal scale in (d), in which liquid flow vectors are plotted over the liquid saturation distribution in (b). A reference vector representing a flow rate of 0.05 m/y is located at the bottom of the plot in (d). 18

10 Volume fraction of quartz, chalcedony, and amorphous silica precipitated in the fracture plotted as a function of fracture volume fraction for a matrix porosity $\phi_m = 0.1$. A volume fraction of one represents complete filling of the fracture, assuming that the fracture was initially devoid of solid filling. . 20

11 Porosity profile into the rock matrix for $q = 300$ m^{-1} (upper curves) and $q = 112$ m^{-1} (lower curves). Red corresponds to a zero-flux boundary condition, blue to a fixed concentration boundary condition, and green to an infinite system. All three curves coincide for $q = 300$ m^{-1}. 33

A NATURAL ANALOGUE FOR THERMAL-HYDROLOGIC-CHEMICAL COUPLED PROCESSES AT THE PROPOSED NUCLEAR WASTE REPOSITORY AT YUCCA MOUNTAIN, NEVADA

Peter C. Lichtner
Gordon Keating
Bill Carey

ABSTRACT

Dike and sill complexes that intruded tuffaceous host rocks above the water table are suggested as natural analogues for thermal-hydrologic-chemical (THC) processes at the proposed nuclear waste repository at Yucca Mountain, Nevada. Scoping thermal-hydrologic calculations of temperature and saturation profiles surrounding a 30–50 m wide intrusion suggest that boiling conditions could be sustained at distances of tens of meters from the intrusion for several thousand years. This time scale for persistence of boiling is similar to that expected for the Yucca Mountain repository with moderate heat loading. By studying the hydrothermal alteration of the tuff host rocks surrounding the intrusions, insight and relevant data can be obtained that apply directly to the Yucca Mountain repository and can shed light on the extent and type of alteration that should be expected. Such data are needed to bound and constrain model parameters used in THC simulations of the effect of heat produced by the waste on the host rock and to provide a firm foundation for assessing overall repository performance.

One example of a possible natural analogue for the repository is the Paiute Ridge intrusive complex located on the northeastern boundary of the Nevada Test Site, Nye County, Nevada. The complex consists of dikes and sills intruded into a partially saturated tuffaceous host rock that has stratigraphic sequences that correlate with those found at Yucca Mountain. The intrusions were emplaced at a depth of several hundred meters below the surface, similar to the depth of the proposed repository. The tuffaceous host rock surrounding the intrusions is hydrothermally altered to varying extents depending on the distance from the intrusions. The Paiute Ridge intrusive complex thus appears to be an ideal natural analogue of THC coupled processes associated with the Yucca Mountain repository. It could provide much needed physical and chemical data for understanding the influence of heat released from the repository on the tuff host rock and for THC modeling studies of the repository. Many other such intrusive complexes exist at the Nevada Test Site and in other parts of the world that could provide an extensive data set for understanding and predicting the behavior of the Yucca Mountain repository, for which the Paiute Ridge complex is just one example.

1 INTRODUCTION

Considerable uncertainty exists regarding the degree of mineral alteration that may occur in the tuffaceous host rock at the proposed repository at Yucca Mountain, Nevada, in response to the release of heat following emplacement of high-level nuclear waste (HLW). Attempts to quantify the extent of alteration, based on thermal-hydrologic-chemical (THC) modeling efforts, are often characterized as "data starved." This is because of the difficulty in supplying values for the necessary physical, thermodynamic, and kinetic parameters needed for the complex computer models that incorporate THC coupled processes. But an even more fundamental difficulty is understanding the prevailing physical and chemical processes in the first place, so that they may be properly incorporated into a model. Seldom, if it all, has it been possible to predict *a priori* the behavior of complex geochemical systems from numerical models alone. Complex THC processes such as might be involved at the proposed Yucca Mountain repository present an even greater challenge.

To properly model mineral alteration processes in the highly fractured tuff host rock, mineral concentrations and associated surface areas in fractures and rock matrix must be distinguished, and kinetic rate constants—including nucleation kinetics associated with the transformation of metastable phases—must be known. In addition, mineral alteration may result in significant changes to hydrologic and transport properties such as permeability, porosity, and tortuosity of the repository host rock. Quantification of these changes is poorly understood. Formation of mineral alteration zones on the order of millimeters to centimeters could strongly impact the hydrologic properties of the repository host rock. For example, fractures could become filled with silica minerals, forming a low permeable zone, or cap rock, above the repository. Alternatively, the rock matrix bordering fractures could become sealed, thus reducing or preventing matrix imbibition and creating fast pathways for infiltrating water to reach the repository. Only natural analogues provide a means of investigating the slow geologic processes characteristic of the repository which take place over long time spans. Modeling alone, in its present state, does not appear capable of predicting mineral alteration of metastable phases at relatively low temperatures of 100°C or less, and small length scales on the order of millimeters to centimeters, that are involved.

Regardless of whether mineral alteration in the repository host rock is beneficial or detrimental to the integrity of the repository, the potential changes in physical and chemical properties of the host rock creates significant uncertainty in performance assessment models for estimating the movement of radionuclides from the repository to the accessible environment. The purpose of this white paper is to suggest that a resolution of THC near-field issues can be obtained through analysis of various intrusive complexes hosted in tuffaceous rock above the water table. Recently, Matyskiela (1997) proposed the Papoose Lake sill (on the northern edge of the Paiute Ridge intrusive complex) as a possible natural analogue of the proposed Yucca Mountain repository. However, the analysis and data presented by Matyskiela (1997) raise a number of unanswered questions that need further study as to the extent of host rock alteration due to the Papoose Lake sill.

Preliminary modeling studies presented in this white paper suggest that the basaltic intrusions into unsaturated tuff at the Paiute Ridge intrusive complex produced thermal, hydrologic, and chemical effects analogous to those being hypothesized for the Yucca Mountain repository. Two-phase numerical simulations accounting for flow of liquid water, water vapor, and air strongly suggest that at distances of tens of meters from the larger intrusions within the complex (width $\geq$30 m), prolonged boiling conditions were established for time spans of several thousand years. By careful observation of mineral alteration in these two-phase regions, the behavior of the proposed Yucca Mountain repository emplaced in a tuffaceous host rock can be evaluated. By combining field observations of Paiute Ridge and other intrusive complexes with selective modeling studies, it is expected that a clear picture can emerge as to the extent of alteration that can be expected at the proposed Yucca Mountain repository.

2 THC COUPLED PROCESSES ASSOCIATED WITH THE PROPOSED YUCCA MOUNTAIN REPOSITORY

The tuffaceous host rocks at Yucca Mountain exist in a metastable state and are composed primarily of volcanic glass, silica polymorphs (cristobalite, tridymite, and opal-CT), feldspars, zeolites, clays, and calcite. An important question is to ascertain whether and at what rate this metastable assemblage will revert to a thermodynamically stable configuration as a result of heat introduced by the repository. This transformation can be accelerated with the addition of heat in the presence of liquid water in an otherwise closed system. Considerable controversy exists in estimating the impact that heat produced by the decaying nuclear waste will have on the repository's performance over time.

It is important to distinguish between changes in the near-field environment that take place in a closed system and changes due to fluid fluxes as consequences of the heat generated from radioactive decay. Formation of heat pipes characterized by counterflow of liquid and vapor—with evaporation taking place at one end of the heat pipe and condensation of water vapor at the other—result in degassing of CO_2 and a consequent increase in pH and purging of oxygen (Lichtner and Seth, 1996). Liquid water in the condensate zone is relatively dilute, with reduced pH and chloride concentrations when compared to the ambient groundwater composition. Within the heat pipe zone, the temperature is near boiling at atmospheric pressure. Salts are expected to form in the dry-out zone (in the very near-field region close to drifts containing the waste) where complete evaporation takes place. High salinities could result during the rewetting phase of the repository, depending on the rate at which liquid water comes in contact with the deposited salts. It is not clear, however, what effect, if any, these fluid fluxes will have on mineral alteration. This thermal period is expected to last for, at most, several thousand years with relatively low liquid fluxes (Lichtner and Seth, 1996; Hardin, 1998).

Possible scenarios—based on THC simulations of mineral alteration resulting from

heat released from the decay of radioactive waste—range from little or no alteration at all, to extensive alteration with the formation of a silica cap above the repository and alteration of feldspars, silica polymorphs, and glass to zeolites and clay minerals (Hardin, 1998; Whitbeck and Glassley, 1998; Nitao, 1998). The latter strong alteration scenario could result in significant changes in porosity and permeability of the repository host rock that could affect its performance, both favorably and unfavorably. The formation of a silica cap requires the assumption of an extremely small fracture porosity that may not be valid. The strong alteration scenario is supposed to take place over relatively short time spans, on the order of several thousand years, and at relatively low temperatures, near the boiling point of water under atmospheric pressure. These conditions raise serious questions as to the validity of this scenario. At such low temperatures, nucleation kinetics can inhibit certain reactions from taking place, such as precipitation of quartz, zeolites, or clays, even though such reactions are possible thermodynamically. As a consequence, there exists significant uncertainty as to which reactions will actually take place. Even if such reactions do take place, the rate at which they might occur is highly uncertain because of the lack of knowledge of the hydrodynamically accessible surface area of the minerals involved. Generally, silicate minerals react relatively slowly at low temperatures, requiring geologic time spans (>10,000 yr) before significant alteration can take place.

Typically, THC calculations are performed using various forms of the dual continuum model (DCM) to distinguish between fracture and matrix flow systems. The different DCMs are distinguished by the number of matrix nodes and their connectivity (Lichtner, 1999b). Although fracture apertures used in DCMs can be on the order of millimeters or less, matrix block sizes are generally quite large—on the order of a meter to half a meter or larger—governed by the fracture spacing. Employing a DCM with a single matrix node of this size associated with each fracture node, it would be virtually impossible to describe processes taking place in the rock matrix at the millimeter to centimeter scale. DCMs which attempt to discretize the rock matrix are computationally intensive and have not been used extensively in THC models applied to the Yucca Mountain repository.

3 PAIUTE RIDGE INTRUSIVE COMPLEX AS A NATURAL ANALOGUE

3.1 Paiute Ridge Geology

The Paiute Ridge intrusive complex is located on the northeastern boundary of the Nevada Test Site, Nye County, Nevada, within the Halfpint Range (Figure 1). The intrusive complex is located in a fault-bounded valley surrounded by Paiute Ridge, Slanted Buttes, and Carbonate Ridge. The geology of the region was mapped by Byers and Barnes (1967) and remapped and studied in greater detail by Goff and others in 1995 (Goff, 1995; Valentine et al., 1998) (Figure 1). Bedrock consists of Ordovician limestone paleohills (fault

blocks and erosional landforms) that have been locally buried by late Tertiary ash flows and fallout tephra. The pyroclastic deposits include material erupted from the Silent Canyon, Claim Canyon, and Timber Mountain calderas of the southwestern Nevada volcanic field (SWNVF), located approximately 25 km to the west, and possibly other, older eruptive centers. Pyroclastic strata identified in the Paiute Ridge area include the Pahranagat Formation (18–22 Ma), Volcanics of Oak Spring Butte (15 Ma), Wahmonie Formation (13 Ma), Calico Hills Formation (12.9 Ma), Paintbrush Group (12.7–12.8 Ma), and the Timber Mountain Group (11.45–12.5 Ma) (Sawyer et al., 1994; Goff, 1995; Warren, 1995; Valentine et al., 1998). Many of these units are found at Yucca Mountain, 40 km to the southwest. Other regional strata in the 13–15 Ma range most likely are also present but have not been identified (Warren, 1995).

The carbonate strata and mid-Miocene tephra have been faulted and tilted to form elongated blocks of a north-northwest trending graben system 15–20 km long and 4–8 km wide (Valentine et al., 1998). East-west extensional deformation in local areas of the Great Basin reached a maximum in the mid-Miocene time period, concurrent with the eruption of large volumes of tephra (on the order of 1000 km^3 per eruption) from calderas of the SWNVF (Sawyer et al., 1994; Minor, 1995). The eastern portions of the SWNVF experienced post-eruptive extension as well (Sawyer et al., 1994). Normal fault offsets observed in both the lower Paleozoic carbonate strata and the mid-Miocene tephra in the Pauite Ridge area are consistent with syn- and post-eruptive regional extension. Late-Miocene intrusive units, discussed below, show little, if any, offset associated with extensional faulting.

The bounding faults of this graben system formed pathways for magma ascent in late Miocene, when mafic alkaline (hawaiite) magma intruded and formed dikes, sills, and saucer-shaped lopolithic intrusions within the tuffs and carbonates (Crowe et al., 1983; Carter Krogh and Valentine, 1996). Results of petrologic studies (summarized in Carter Krogh and Valentine, 1996), radiometric age dating (Crowe et al., 1983; Ratcliff et al., 1994), and paleomagnetic analysis (Ratcliff et al., 1994) indicate that the basaltic magma intruded in a single magmatic pulse; no cross-cutting relationships have been observed among the dikes and sills in the field (Valentine et al., 1998; Carter Krogh and Valentine, 1996). The age of the intrusions is 8.5–8.6 Ma (Crowe et al., 1983; Ratcliff et al., 1994). The intrusions formed as dikes that dilated existing faults; continued magmatic injection resulted in flow focusing into plugs, and subhorizontal diversions into sills and lopoliths. The original depth of the intrusions exposed at Paiute Ridge is on the order of 150–250 m, based on exposures of scoria and extrusive basalt preserved on ridgetops (Crowe et al., 1983; Carter Krogh and Valentine, 1996) (Figure 2). The shallow depth and magmatic overpressure of the largest subhorizontal sills caused them to deflect the overlaying tuff to form domed lopoliths (Crowe et al., 1983). Several of these sill-like intrusions occur along the contact between tuffs of the Paintbrush and overlying Timber Mountain groups, producing concordant and discordant subhorizontal geometries (Crowe et al., 1983). The discordant intrusions often remain subhorizontal as they cross gently dipping (20°) beds within the tuff. The intrusions are generally massive and dense and form platy, contact-parallel cooling joints along the contact. Localized areas of scoria and vesicular dike margins signify

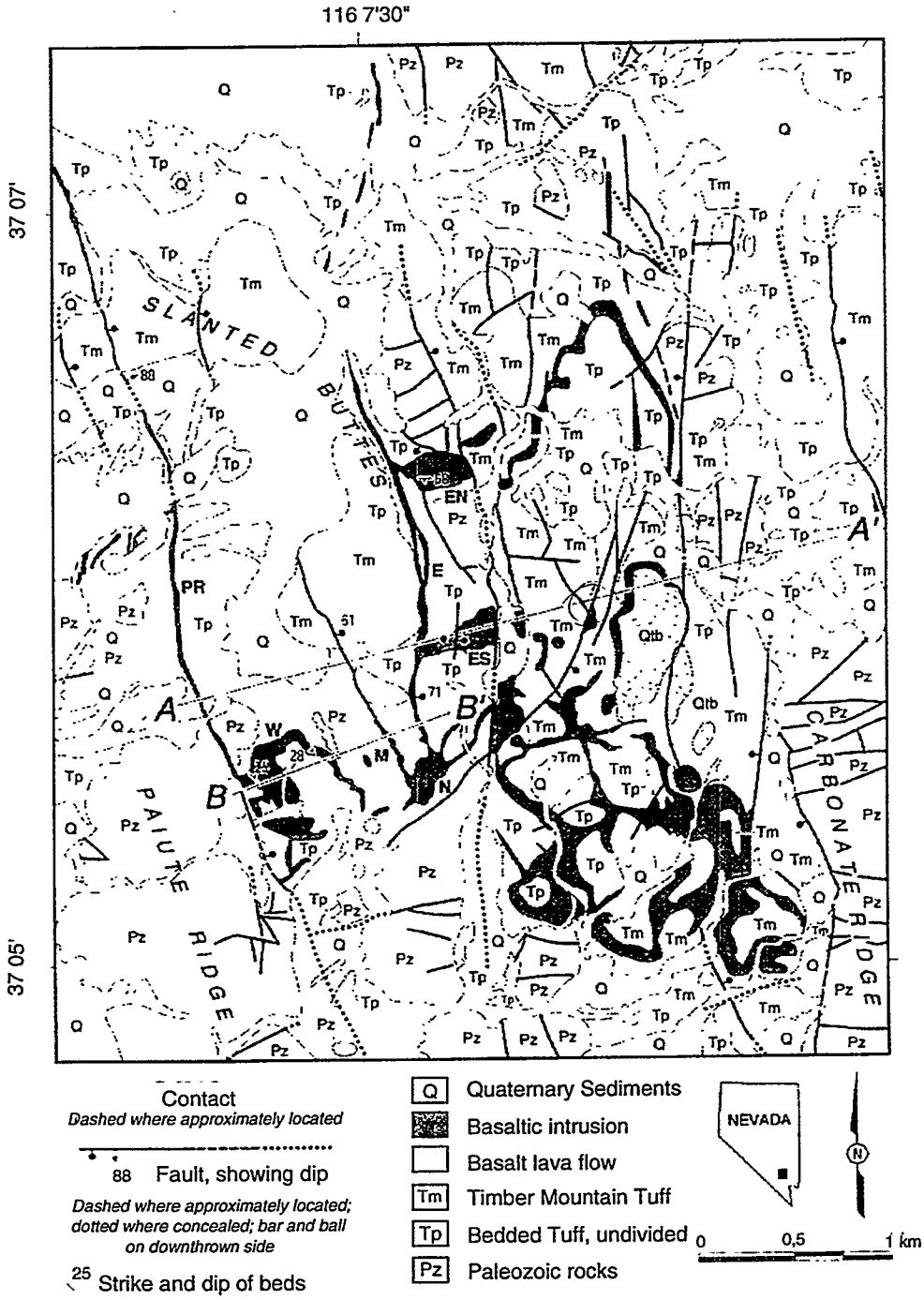

Figure 1: Geologic map of the Slanted Buttes, Half Pint Range, Nevada. Inset map shows the location of Slanted Buttes. The geologic map indicates the sample locations of tuffs intruded by dikes and sills. Reprinted from Valentine et al., (1998) Figure 5.19, page 5-45.

the areas where the intrusions approached the surface (Valentine et al., 1998; Carter Krogh and Valentine, 1996).

Serendipitously, the thermal event caused by the emplacement and cooling of the mafic intrusions at Paiute Ridge occurred during a reversal in the Earth's magnetic field, and the magnetic minerals in the intrusions and host rock captured details of its evolution. The paleomagnetic character (directional and intensity variations) of this reversal has been studied

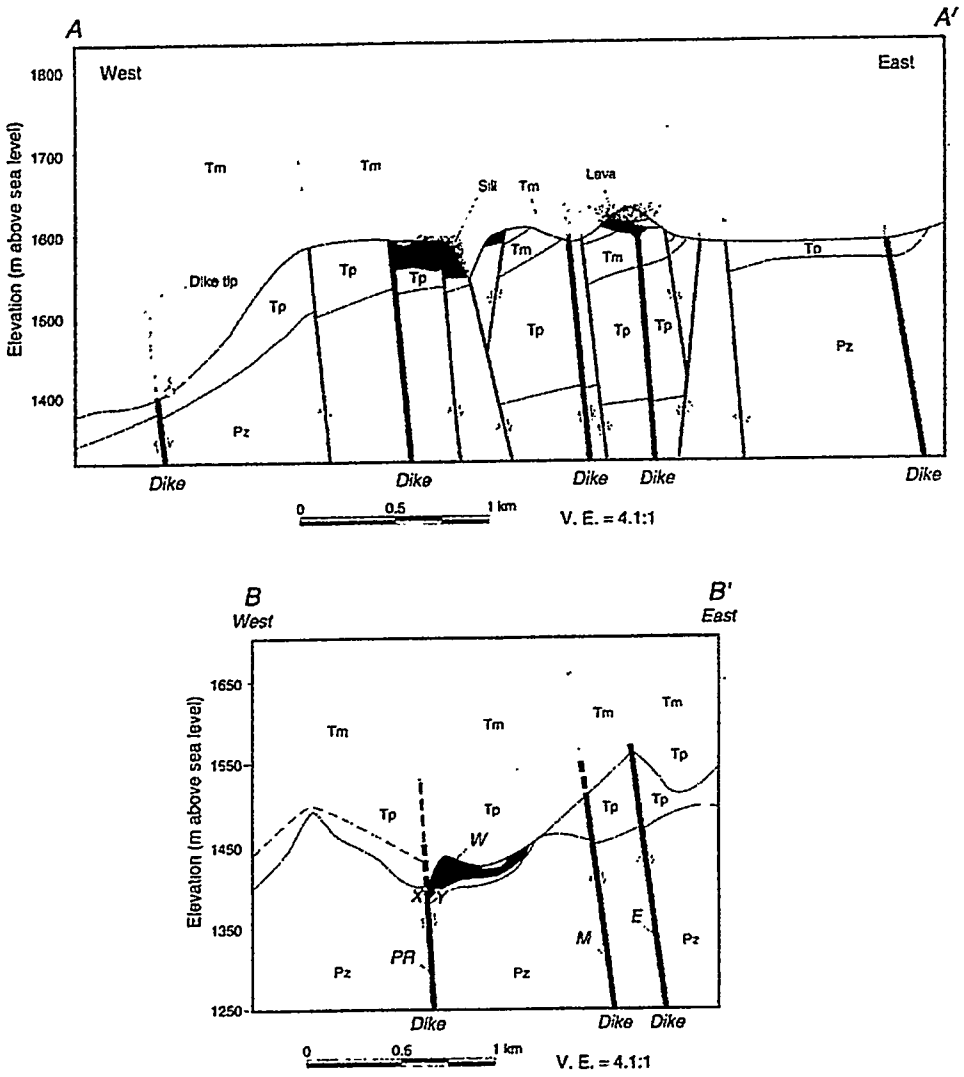

Figure 2: Cross sections through Paiute Ridge area (A-A′ and B-B′ in Figure 1) showing present day topography and geology, with inferred topography (dashed) at the time of basaltic activity. Legend is the same as in Figure 1. Reprinted from Carter Krogh and Valentine (1996).

in detail by Ratcliff and Geissman (Ratcliff et al., 1994) at the University of New Mexico. These workers have studied the magnetic character of both the intrusions and the fused, tuffaceous host rocks to determine that the dipole portions of the geomagnetic field tracked from normal to reversed polarity through a well-defined west-Pacific longitudinal belt (Ratcliff et al., 1994; Geissman, 1998, personal communication). Further work is ongoing to better understand the character and duration of the transition (Keating and Geissman,

1998). The results of the paleomagnetic and numerical thermal modeling studies of this reversal will have bearing on the study described in this white paper: both provide information about the extent and temporal evolution of the thermal aureole surrounding the intrusions.

The tuffs that form the host rocks for the intrusions are generally nonwelded to poorly welded and include massive, pumice- and ash-rich ignimbrites (ashflow tuffs) and bedded, well-sorted pumice- or ash-fall layers. Variable alteration associated with the original cooling of the deposits resulted in large variability in the vitric vs. zeolite content of the tuffs. The geologic map by Byers and Barnes (1967) delineates tuff stratigraphy and intrusion geometries and attempts to identify areas of "alteration" (associated with the intrusions) and "zeolitization" (of any origin). However, these characterizations must be reevaluated in light of the revised stratigraphic definitions of the study area developed by Goff and others (Goff, 1995; Valentine et al., 1998) and Warren (1995). This newer mapping redefines several parts of the study area, reassigning strata termed "Paintbrush Tuff-Undivided" and "Altered Tuff" into older units (e.g., Calico Hills Formation, Wahmonie Formation, Tunnel Formation, Volcanics of Oak Spring Butte) with distinctly different petrographic and alteration characteristics. The age, primary mineralogy and textural character, and degree and origin of alteration in these rocks has come into question and must be well established before meaningful interpretations can be made regarding the timing and nature of the observed alteration of the tuff (and its relationship, if any, to the intrusions). Some of the existing published research into the alteration of the tuff related to the intrusive event (Matyskiela, 1997) relied on the older map and stratigraphic designations of Byers and Barnes (1967), which has been found to be in error in several parts of the Paiute Ridge study area.

The physical effects of the intrusions on the surrounding tuffaceous host rock are fairly uniform, despite lithologic changes in the host rock and the varying size of the intrusions. The tuff within 0.5 to 1.0 m of the contact is commonly completely fused to a gray to black vitrophyre. This zone often contains abundant contact-parallel, anastamosing joints. The original texture of the tuff in this zone is overprinted by contact-parallel (often normal to original bedding) fiamme (flattened, elongated pumice). From 1 to 3 m from the contact, the degree of contact welding decreases to a sintered texture or to the original, nonwelded character, with a progressive decrease in the degree of flattening of the pumice lumps and decreasing hardness or induration of the rock. The primary texture of the host tuff affects the texture of the resulting vitrophyre: fine-grained, ashy tuff produces a dense, massive, "hornfelsed" vitrophyre; coarser, more pumice-rich tuff results in coarse-grained, foliated vitrophyre and densely welded tuff with abundant, well-developed fiamme; crystal-rich tuff is transformed into a "salt-and-pepper" textured vitrophyre that easily can be mistaken for diorite. These variations in primary texture must be identified before the secondary effects of the contact metamorphism can be analyzed.

Due to the nature of weathering and erosion in the arid southwest, the best exposures of the intrusive complex and its contact metamorphic aureole are along the contacts between

intruding basalt and tuff host rocks. The interior of the intrusions is often coarsely crystallized (poikilitic), pebbly, and highly eroded, such that the intrusions are only exposed along the contact. Similarly, the host tuff is originally nonwelded or poorly welded and is only resistant to weathering where it is densely welded along contacts with the basalt. The resulting landforms are rolling hills of slope-forming tuff and intrusion interiors with low (1–3 m) hogbacks signifying the contact zones. These resistant exposures generally extend only 1–3 m from the contact in either direction, but more extensive exposures occur in dry washes that cut through the contact zone.

In thin section, the thermal aureole is characterized by transformation of tuff to completely annealed vitric material against the contact, with devitrification and partial alteration of glass to clays beginning about 2 m from the contact (see Figure 3). Clays found at 2 m include higher-temperature phases (e.g., illite, maximum of 15% of sample volume), and the character of the clay appears to vary gradually with distance, so that the common clays are lower-temperature phases (e.g., montmorillonite) by 3–5 m distance. Devitrification of the volcanic glass shards and pumice to silica phases (cristobalite) and K-rich feldspars begins by 2 m distance from the contact and increases in intensity with increasing distance. This observed pattern of alteration is consistent with the development of a dry-out zone in the host rock nearest the intrusion and increasing alteration in the zone of boiling and water condensation that extends tens of meters from the dike (described in more detail in the hydrothermal modeling section below). This preliminary characterization of the variation in host rock alteration is based on field observations and thin section and laboratory analysis ata small number of aureole exposures, and it must be quantified by additional petrography and laboratory analysis (e.g., X-ray diffraction). In addition, as mentioned above, the variation in primary host rock stratigraphy with distance from the contact strongly affects the nature of the final alteration in the aureole. As a consequence, the primary stratigraphy must be identified with confidence through additional field and laboratory analyses before the extent of hydrothermal alteration resulting from emplacement of the dike can be ascertained.

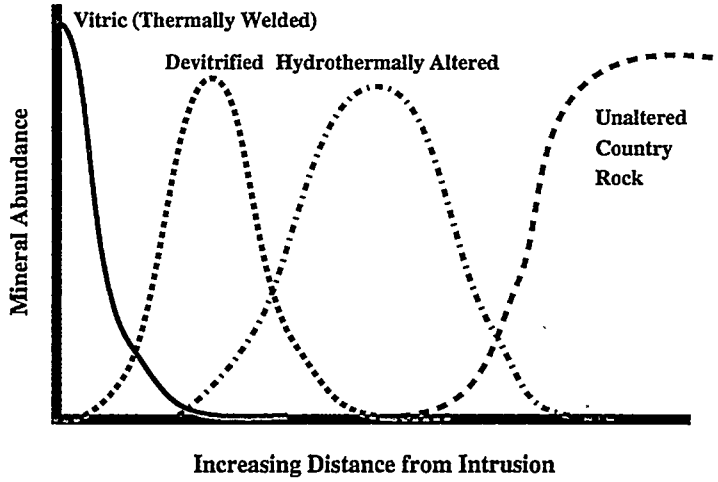

Figure 3: Schematic illustration of a possible mineral alteration paragenesis adjacent to a dike intruded into vitric tuff.

The geochemical nature of the contact metamorphic aureole has been studied only briefly by G. WoldeGabriel (Valentine et al., 1998). In one dike-contact locality, tuff mineralogy within approximately 15 m of the contact shows the decreasing effects of contact metamorphism away from the dike. The abundance of volcanic glass displays a marked decline approaching the contact, while the abundance of feldspar and cristobalite increases; this is a clearly developed trend in devitrification within 15 m of the contact. Other alteration minerals, such as amorphous silica, clays, and calcite, are locally present, but they show no clear trends with distance in the thermal aureole.

Evidence of transport and deposition of silica and other phases in fractures and matrix is ambiguous. Local fractures are abundant in the contact basalt and tuff, and fracture spacing increases from 1–10 cm in the vitrophyre to about 1 m at a distance of 1 to 3 m from the contact. Localized (millimeter-scale) bleaching along joints in the contact welded tuff disappears within 1 m, and fractures observed at greater distances from the contact that show no alteration along their margins may be a result of erosional unloading and weathering.

A zone of reddening in the tuff host rock commonly occurs within tens of meters from the contact. This change in coloring, from the original white to tan color, is likely due to oxidation of iron within the tuff rock. At one locality, 2-cm reddened veins occur within 3 to 12 m from the contact. These veins appear to be the result of alteration of the matrix in the vicinity of fractures. The fractures are now filled with silica polymorphs. It is unclear, however, whether this alteration formed under boiling conditions with liquid water present or whether it occurred at higher temperatures.

Although fracture-matrix mineralization has been reported in some localities (Matyskiela, 1997), such features are uncommon and merit more thorough investigation in the Paiute Ridge study area. WoldeGabriel described a discontinuous 10-cm, light green opaline layer located in baked tuff (Figure 4) about 1 m below a large basaltic sill (Valentine et al., 1998). The presence of a thick zone of amorphous silica in the vicinity of the intrusion is intriguing; however, the origin of the opal is highly ambiguous, since it formed parallel to bedding within the tuff and subparallel to the basal contact of the sill. The host tuff in this area is part of the base of the Paintbrush Group or the top of the Calico Hills Formation; the latter formation has been found to have extensive diagenetic alteration to zeolites and amorphous silica (including opal) in other localities (Broxton et al., 1987) due to variable exposure to groundwater in the intervening 12.9 Ma since it was deposited. The presence of minor amounts of the zeolite clinoptilolite in both glassy vitrophyre and completely devitrified tuff, located equal distances beneath a sill, suggests that the zeolitization occurred prior to intrusion and was not related to devitrification and alteration associated with the contact metamorphic event (Valentine et al., 1998).

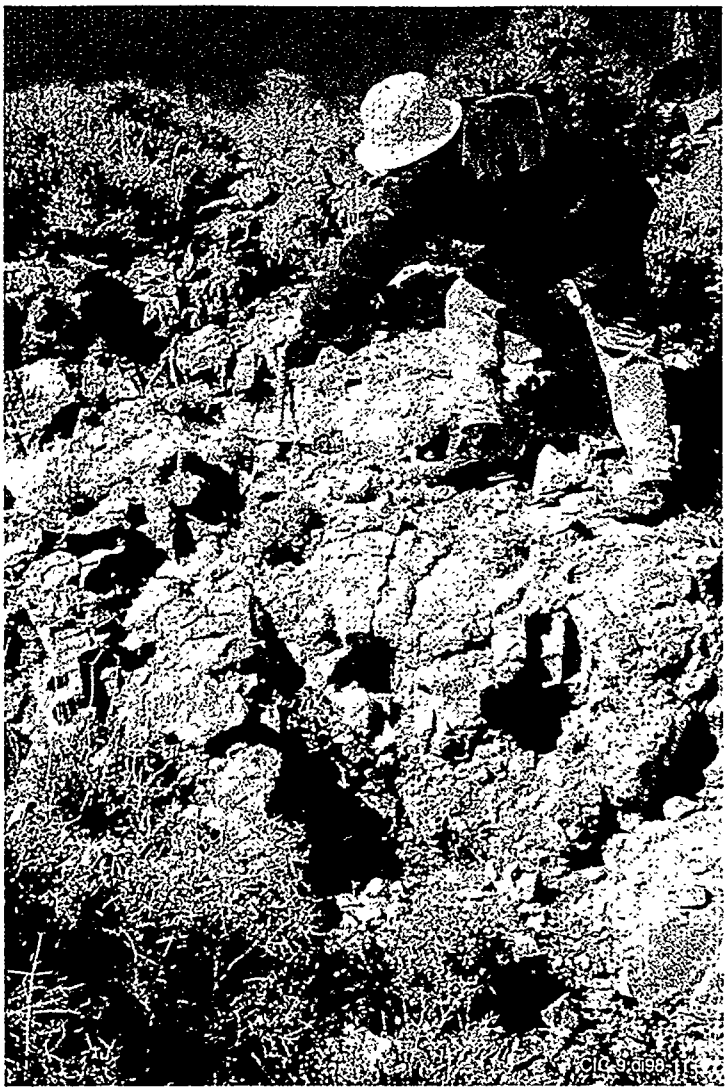

Figure 4: Field observation of a 10 cm opal alteration zone (located behind rock hammer) occurring below a basaltic sill (not visible). Photo used with permission of WoldeGabriel.

3.2 Hydrothermal System

In order for the Paiute Ridge intrusive complex to serve as a natural analogue for the Yucca Mountain repository, it is necessary to demonstrate that the time-temperature-saturation history surrounding an intrusive sill is similar to that predicted for the repository. The amount of heat stored in the intrusion is directly proportional to its width. Typical widths in the Paiute Ridge intrusive complex vary from tens to hundreds of meters. The typical emplacement temperature of a basaltic intrusion is approximately 1000°C to 1200°C. This temperature is considerably higher than the maximum temperature of about 300°C estimated for the repository, and thus the region very near to the intrusion cannot be expected to correspond to repository conditions. However, farther away from the intrusion, the temperature can be expected to be buffered at the boiling temperature of water under atmospheric conditions. In this region, evaporation and condensation processes should be

very similar to those encountered in the proposed Yucca Mountain repository. Very likely, heat-pipe effects could have occurred with counterflow of liquid and vapor that were similar to those predicted to occur above and below the repository.

To estimate the thermal evolution of host rocks surrounding an intrusion emplaced above the water table, it is essential to take into account the two-phase behavior of the system. Latent heat of solidification of the intrusion is neglected, because this process is relatively fast compared to the time required for the intrusion to reach ambient conditions. Preliminary calculations were performed using the computer codes FEHM (Zyvoloski et al., 1997) and FLOTRAN (Lichtner, 1999a). Both FEHM and FLOTRAN are capable of describing two-phase nonisothermal fluid flow in variably saturated media. The version of FEHM used for the calculations in this report was modified by Keating (Keating et al., 1998) to incorporate a revised equation of state for water for the high temperature conditions resulting from the intrusion.

An equivalent continuum representation of the host rock is used in the scoping calculations. This is considered adequate for determining the thermal cooling and bulk saturation history. A one-dimensional (1-D) model is considered of a semi-infinite medium representing the host rock in contact with the intrusion (see Figure 5). This is a simplified model in which the effects of gravity and infiltration are neglected. By symmetry, only half of the dike width need be modeled. A 50 m wide completely dry intrusion with an initial temperature of 1200°C is assumed to be emplaced instantaneously into unsaturated tuff at ambient temperature and pressure. FEHM and FLOTRAN gave essentially identical results for saturation, pressure, and temperature in the calculations presented in this report.

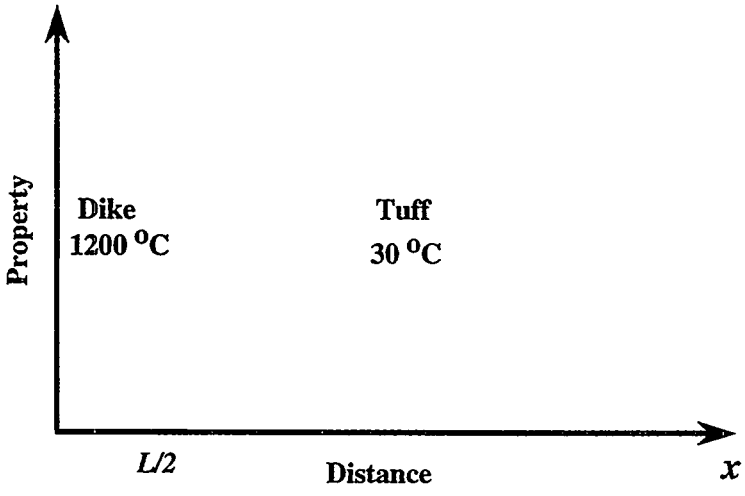

Figure 5: Schematic diagram of a one-dimensional simulation indicating the initial temperature of the intrusion and tuff country rock.

Rock properties and initial and boundary conditions used in the calculations for the equivalent continuum model are listed in Table 1. The values used for density, specific heat, and thermal conductivity for basalt are typical for basalts as listed in Drury (1987).

Table 1: Hydrothermal Model Parameters

Property	Symbol	Units	Mafic Intrusion	Tuff Country Rock
fracture permeability	κ_f	m^2	2.74×10^{-9}	2.74×10^{-9}
matrix permeability	κ_m	m^2	1.0×10^{-20}	4.66×10^{-14}
fracture porosity	ϕ_f	—	6.69×10^{-5}	6.69×10^{-5}
matrix porosity	ϕ_m	—	0.05	0.47
density	ρ_r	$kg\ m^{-3}$	2830	2410
specific heat	C_p	$J\ kg^{-1}\ K^{-1}$	1010	1100
thermal conductivity	C_{dry}	$J\ s^{-1}\ m^{-1}\ K^{-1}$	1.93	1.93
thermal conductivity	C_{wet}	$J\ s^{-1}\ m^{-1}\ K^{-1}$	0.61	0.61
gaseous diffusivity	D	$m^2\ s^{-1}$	2.13×10^{-5}	2.13×10^{-5}
temperature exponent	θ	—	1.8	1.8
tortuosity	τ	—	1.0	1.0
residual saturation	s_r	—	0.04	0.04
van Genuchten parameter	α_f	Pa^{-1}	8.92×10^{-4}	8.92×10^{-4}
van Genuchten parameter	α_m	Pa^{-1}	4.15×10^{-5}	4.15×10^{-5}
van Genuchten parameter	λ_f	—	0.449	0.449
van Genuchten parameter	λ_m	—	0.327	0.327
initial temperature	T_0	°C	1200	30
initial saturation	s_l^0	—	0.0	0.4

Very small values for porosity and permeability for basalt were chosen to simulate an essentially impermeable intrusion. The "tuff" values are representative of the Paintbrush tuff, nonwelded (PTn) at Yucca Mountain (approximately analogous to the nonwelded tuffs at Paiute Ridge). Values for van Genuchten parameters (fracture/matrix "effective continuum") are means for PTn values in Wu et al. (1997). Thermal properties of tuff are from Francis (1997). Values for density and porosity are from Peters et al. (1984). Saturation values ranging from 0.4–0.6 are observed for the PTn at Yucca Mountain, and corresponding calibrated model values were taken from Robinson et al. (1997).

The time-temperature histories at different distances from the intrusion for an initial saturation of 0.4 are shown in Figure 6(a), (b), and (c) corresponding to widths of 10 m, 30 m and 50 m. In Figure 7, temperatures above 100°C indicate complete dry-out of the rock, as pressures are nearly atmospheric because the intrusion lies above the water table. Under such conditions, for liquid water to be present, the temperature must lie at or below the boiling point. Following emplacement of the intrusion, liquid water in the tuff host rock begins to boil—with a slight delay in the onset of boiling, depending on the distance from the intrusion. As boiling commences, the temperature is fixed on the boiling curve until all liquid water is removed. At that time, the temperature begins to rise above boiling. After reaching a maximum, the temperature begins to decline as the host rock cools. Capillary forces result in liquid water being sucked towards the hot intrusion, where it evaporates and recondenses further away, producing a condensate zone. Figure 8 shows the saturation

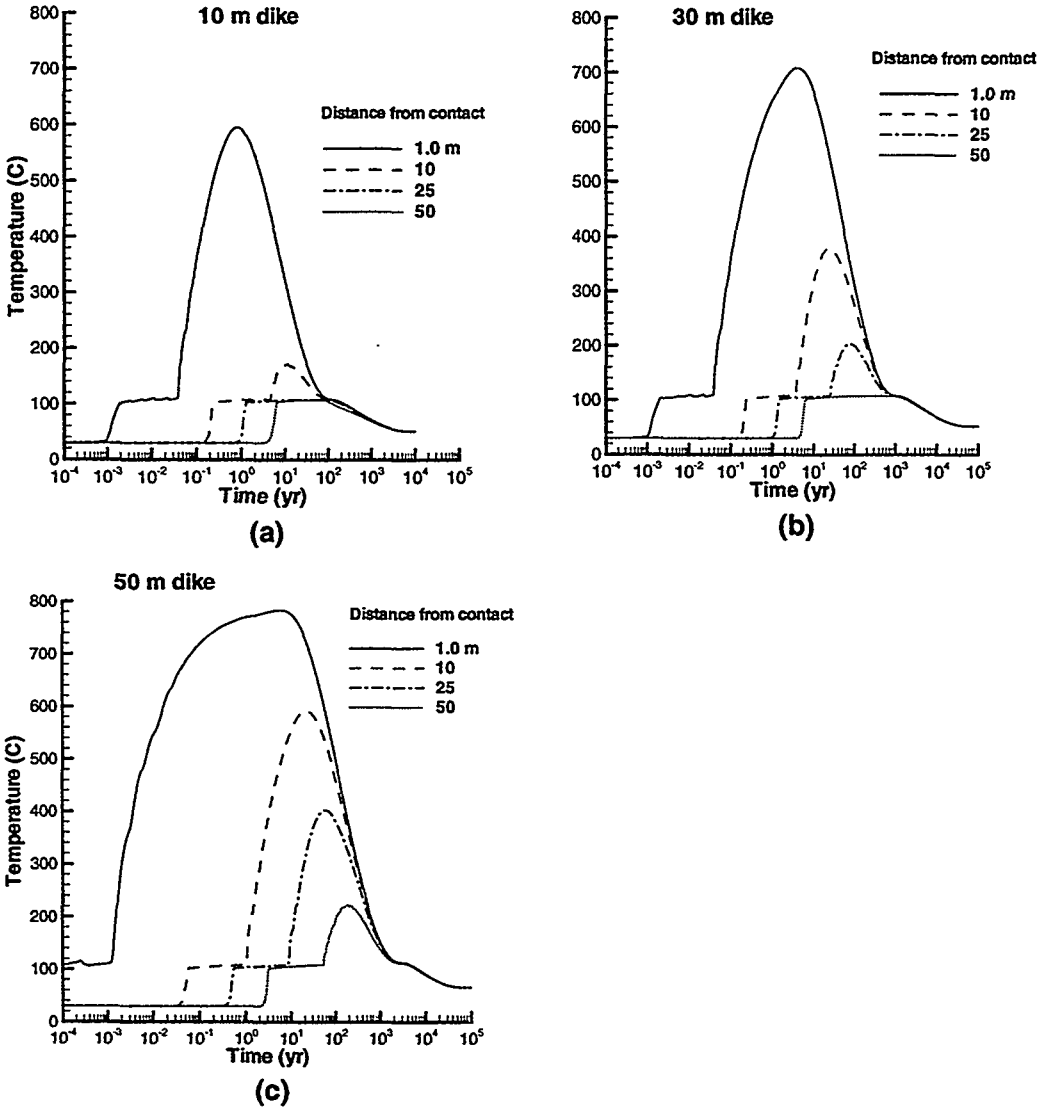

Figure 6: Temperature profiles computed by using an equivalent continuum model with the parameters listed in Table 1 with an initial saturation of 0.4. Results are plotted as a function of time, at fixed distances of 1, 10, 25, and 50 m from the intrusion. Shown are intrusive widths of (a) 10 m, (b) 30 m, and (c) 50 m.

history for different initial saturations of 0.4 and 0.6 and for different distances from the intrusion. Times when the saturation is above ambient saturation indicate the presence of the condensate zone at that particular distance from the intrusion. As the boiling front advances, the condensate zone continuously moves outward with time. Eventually, the saturation becomes zero at any fixed location (<50 m) away from the intrusion when all liquid water has boiled away.

During the cooling period, the temperature eventually drops back to boiling as the host rock begins to resaturate. This effect can be seen by comparing the temperature profiles shown in Figure 7 against the saturation time histories shown in Figure 8. Depending on

the thickness of the intrusion and the distance away from the intrusion, the temperature may remain at boiling for as long as several thousand years. As the intrusion and host rock continue to cool, the temperature gradually decreases over a time period of tens of thousands of years until ambient conditions have finally returned.

By examining Figures 6, 7, and 8, it can be seen that similar behaviors are obtained for the cooling intrusive and the repository. A dry-out zone near the intrusion is formed where temperatures are above the boiling point. Further away from the intrusion, a sustained boiling zone is formed. As can be seen from Figures 6 and 7, temperatures remain near boiling for several thousand years depending on the distance from the intrusion. The duration of the boiling regime is found to be roughly independent of the initial saturation.

To assess the effects of gravity and the nature of vertical flow in the vicinity of mafic intrusions at Paiute Ridge, a preliminary two-dimensional (2-D) model domain was developed. The rectangular flow field is 500 m wide by 500 m deep, with a 15-m-wide zone extending from a depth of 20 m to 280 m along the right side boundary (representing the halfwidth of a 30 m vertical intrusion). This geometry represents a simplification of the upturned western limb of the Papoose Lake sill intruded into nonwelded host tuff. The current ground surface corresponds to a depth in the flow field of 150 m. Preliminary calculations indicate that the effects of the central and eastern portions of the sill that are not included in the model domain have insignificant effect on conditions in the host rock to the west of the intrusion. The system is modeled as an equivalent continuum, including material properties for both fractures and matrix within the sill and host rock. Values for material property parameters are the same as in the 1-D model listed in Table 1. Boundary conditions include no-flow boundaries on the right and left sides, a water table ($s_l = 1$) boundary along the bottom, and 5 mm/yr infiltration across the top. In addition, the top and bottom boundaries are held at constant temperature, pressure, and saturation (10°C, 0.1 MPa, 0.4 and 22°C, 0.1 MPa, 1.0, respectively). The model was run to steady state (without the elevated dike temperature), and the resulting T, p, and s_l distributions were used as initial conditions for the simulation, following emplacement of the hot intrusion. The dike was initialized at 1000°C (rather than at 1200°C as in the 1-D simulations). Initial saturation in the host rock was set at 0.4.

In Figure 9, distributions of temperature, liquid saturation, and liquid flow are displayed at a time of 100 years after the intrusion was emplaced and began cooling. Temperature and saturation profiles are shown in Figure 9(c) as a function of distance from the sill at a depth of 150 m. The thermal effects [Figure 9(a) and (c)] of the sill extend out about 100 m from the contact; the edge of the 2-phase (boiling) zone extends about 55 m from the contact, outside a 20-m wide zone of dry-out in the host rock. The saturation and fluid flow distributions [Figure 9(b) and (d)] also depict the 20 m zone of dry-out in host rock. Beyond the dry zone, the expelled moisture condenses and produces a region of enhanced saturation at the edge of the boiling region (as seen in the results of the 1-D model, Figure 8). The effects of gravity are also evident in the location of maximum saturation near the bottom corner of the intrusion. The fluid flow vectors [Figure 9(d)] depict pore fluid

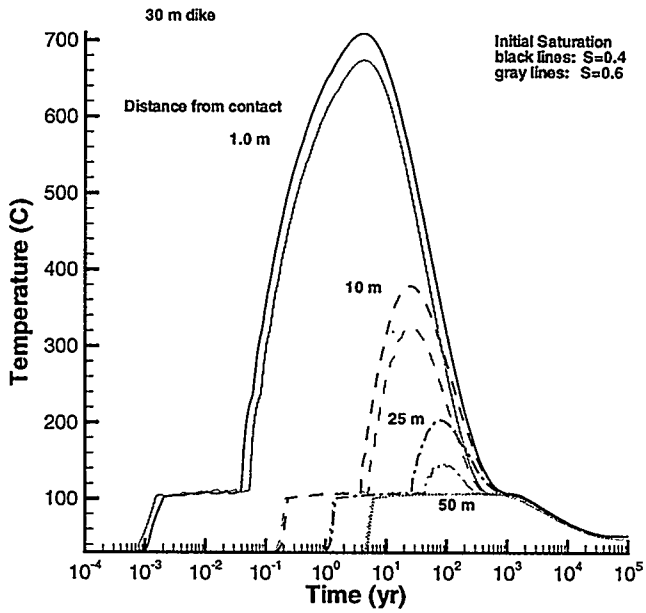

Figure 7: Temperature profiles computed by using an equivalent continuum model, with the parameters listed in Table 1. Initial saturations of 0.4 and 0.6 are used in the calculation. Results are plotted as a function of time, at fixed distances of 1, 10, 25, and 50 m from the intrusion. An intrusive width of 30 m is used in the calculations.

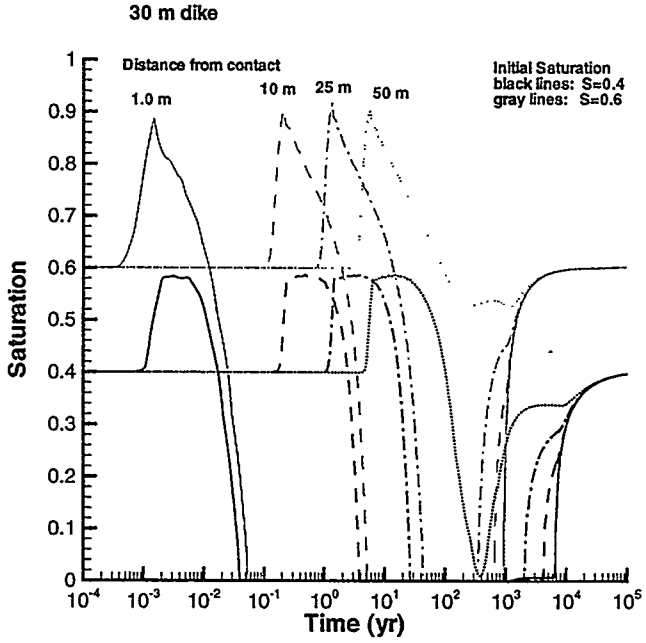

Figure 8: Liquid saturation profiles computed using an equivalent continuum model with the parameters listed in Table 1. Initial saturations of 0.4 and 0.6 are used in the calculations. Results are plotted as functions of time, at fixed distances of 1, 10, 25, and 50 m from the intrusion. An intrusive width of 30 m is used in the calculations.

migration downward, with maximum flow rates in the region of enhanced saturation near the outer edge of the boiling zone. Pore fluid also can be seen migrating laterally through the boiling zone toward the dry-out zone, as stronger horizontal capillary forces overcome the mild effects of gravity.

With the addition of gravity-driven migration of pore water (and the effects of variable meteoric infiltration), the cooling rates simulated in the 2-D model are somewhat faster than those in the 1-D model. Further development of the 2-D model, involving different intrusion geometries, host rock and sill characteristics, and boundary conditions, will provide a better understanding of the evolution of the thermal aureole and implications for conditions near the potential repository.

A more exhaustive study would be needed to consider the sensitivity of the saturation and temperature profiles on other parameters used in the model calculations, including van Genuchten parameters for capillary pressure and relative permeability, permeability, porosity, thermal conductivity, and other parameters. In addition, comparison of different model formulations for fracture-matrix interaction, such as dual continuum models involving connected and disconnected matrix continua, should be performed. Finally, the different stratigraphic units of the host rock need to be included in the model calculations.

3.3 Chemical Reactions

Various chemical reactions are expected to take place as a result of the heat produced from the intrusion and the remobilization of liquid water. Characterization of these reactions is made difficult because of the metastable state of the tuff host rock and the relatively low temperatures ($\sim$100°C) where liquid water is present. Additional complications arise in quantifying mineral surface area and concentrations of primary mineral assemblages. In general, differences between fracture and matrix mineralogy must be taken into account.

Conceptual models for mineral evolution at Yucca Mountain (Carey et al., 1997) suggest that the most likely mineralogical reactions include dissolution of volcanic glass and precipitation of clinoptilolite, clay, and opal-CT; dissolution and precipitation of silica polymorphs (cristobalite, opal-CT, tridymite, and quartz); alteration of feldspar to clays; and finally, reactions involving calcite and zeolites.

A more detailed petrologic study of devitrified and vitric host rocks as a function of distance from the intrusive contact will allow determination of key mineral reactions and hydrologic effects. Field observations at the Paiute Ridge intrusive complex can shed light on which mineral reactions are kinetically possible at Yucca Mountain, which are kinetically insignificant, and which are kinetically or thermodynamically impossible. They can also help to estimate the rates of reactions. Finally, they can be used to determine whether mineral reactions act to increase or decrease matrix or fracture permeability. Field work will provide a testing ground for THC codes and a means for validating the thermodynamic and kinetic models used to calculate mineral reactions. In addition, observations

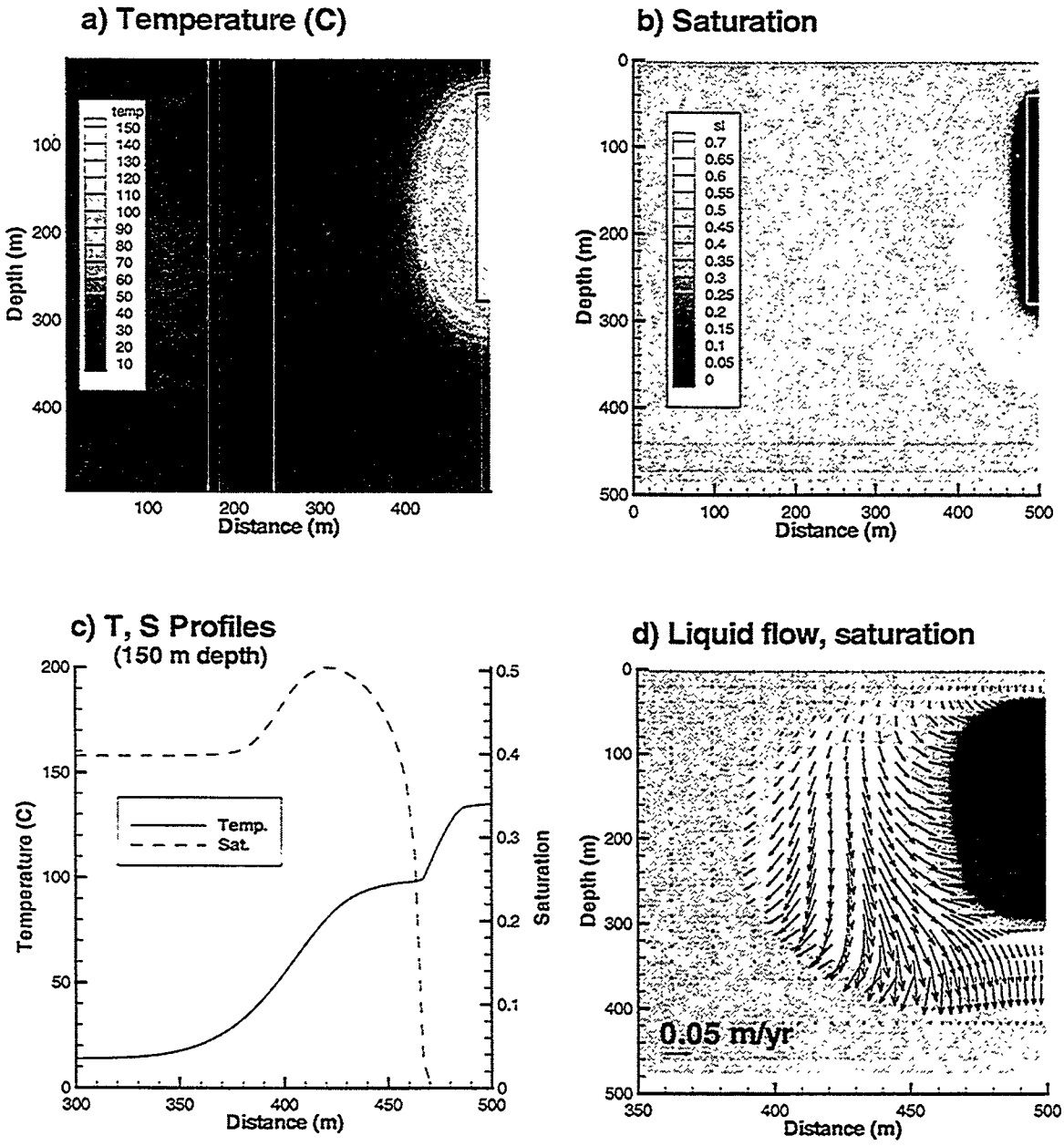

Figure 9: Distributions of (a) temperature, (b) saturation, (c) temperature and saturation profiles at a fixed depth of 150 m, and (d) liquid flow in a two-dimensional flow field surrounding the Papoose Lake intrusion, 100 years after the emplacement of a 1000°C sill. Boundaries include a water table condition along the bottom, 5 mm/yr infiltration along the top, and no-flow sides; see text for a more detailed description of the model domain. The rectangles along the upper right boundary in plots (a) and (b) represent the dimensions of the sill. Note the change of horizontal scale in (d), in which liquid flow vectors are plotted over the liquid saturation distribution in (b). A reference vector representing a flow rate of 0.05 m/y is located at the bottom of the plot in (d).

of fracture-matrix margins may also provide a means for testing and validating porosity/permeability and matrix/fracture interaction models employed in THC codes.

An example of the potential importance of fractures and heat generated by the repository can be seen by considering the following Gedanken experiment. Imagine that the pore fluid in the rock matrix is brought to equilibrium with respect to a particular silica polymorph, such as amorphous silica, at boiling conditions. Further consider that as the fluid in the matrix boils, it escapes into the surrounding fracture network. As the matrix pore fluid is vaporized, it releases its silica content that precipitates in fractures. At issue is the extent to which the fracture can be filled by the silica contained in the matrix pore water. From mass balance considerations, the volume fraction of solid precipitated in the fracture $\phi^f_{SiO_2}$ can be determined from the expression

$$\phi^f_{SiO_2} = \frac{\phi_m \epsilon_f}{1-\epsilon_f} C^m_{SiO_2} \overline{V}_{SiO_2}. \quad (1)$$

In this relation, $C^m_{SiO_2}$ denotes the concentration of silica in the matrix pore fluid at 100°C that is assumed to be in equilibrium with a particular silica polymorph with molar volume $\overline{V}_{SiO_2}$. The fracture volume fraction (the ratio of fracture volume to bulk rock volume) is represented by ϵ_f. Matrix porosity is denoted by ϕ_m. This analysis is dependent on all matrix pore water flashing to steam in the fracture. If this is not the case—for example, a drying front may propagate inward into the matrix, depositing silica within the matrix—then Eq. (1) provides an upper bound on the extent of fracture filling. Results for a matrix porosity of $\phi_m = 0.1$ are shown in Figure 10 for quartz, chalcedony, and amorphous silica. From the figure, it is clear that for a given matrix porosity, the degree of sealing of the fracture depends on the fracture volume fraction ϵ_f and the particular silica polymorph which precipitates. Amorphous silica, with its higher solubility, gives the largest fracture filling, followed by chalcedony and quartz. For complete sealing of the fracture, a very small fracture volume fraction is necessary. Moderate filling could represent fracture coatings that armor the fracture.

4 CRITERIA FOR SELECTING AN INTRUSIVE BODY AS A NATURAL ANALOGUE

Several criteria should be satisfied for an intrusive body to serve as a natural analogue for the Yucca Mountain repository. These should include the following:

- The intrusive must be of sufficient size to produce enough heat to sustain boiling conditions for time spans of several thousand years. Typically, dikes and sills with widths greater than approximately 30 m will be required.
- The intrusive must be emplaced above the water table.

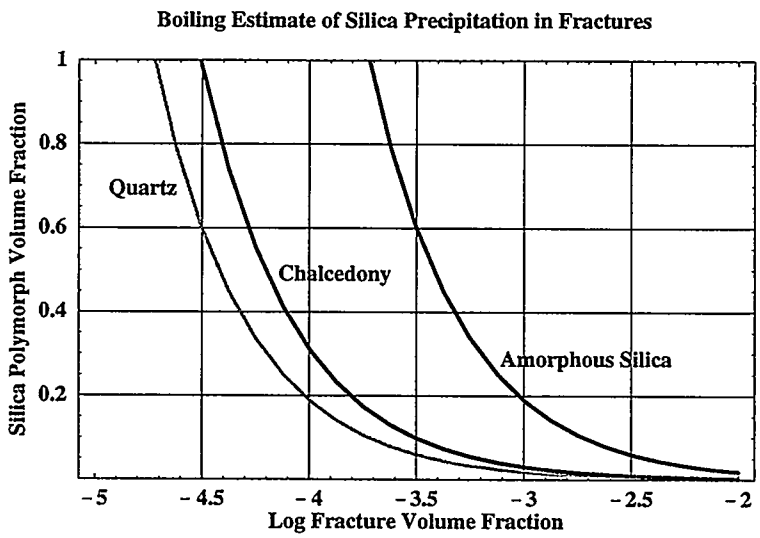

Figure 10: Volume fraction of quartz, chalcedony, and amorphous silica precipitated in the fracture plotted as a function of fracture volume fraction for a matrix porosity $\phi_m = 0.1$. A volume fraction of one represents complete filling of the fracture, assuming that the fracture was initially devoid of solid filling.

- Ideally, the host rock in which the intrusive is emplaced should be a volcanic tuff with composition and physical properties similar to the Topopah Spring stratigraphic unit at Yucca Mountain.

The Paiute Ridge intrusive complex satisfies the first two criteria; however, the tuff host rock in which it has intruded is more similar to the Paintbrush and Calico Hills formations than to the Topopah Spring. The Paintbrush and Calico Hills formations have different chemical and physical properties compared to the Topopah Spring unit. They consist of nonwelded vitric tuffs, whereas the Topopah Spring unit, proposed for the repository, is a densely welded nonvitric tuff. Physical properties, including fracture and matrix porosity and permeability and capillary properties, are different. The chemical composition is also different—the Paintbrush and Calico Hills formations contain glass, compared to the crystalline form of the Topopah Spring. As a consequence, wetting and drying characteristics as well as chemical alteration can be expected to be different. Even so, given the difficulty in finding an exact analogue of the repository host rock, the Paiute Ridge complex will provide answers to many of the unanswered questions associated with THC processes at the repository.

Implementation of the Paiute Ridge intrusive complex as a natural analogue for the Yucca Mountain repository would require additional field work in the area as well as THC modeling studies. Previous field work was primarily concerned with characterizing the unaltered rock before emplacement of the intrusive complex and investigating mineralogic alteration and devitrification in the immediate vicinity of the intrusions. Future work would be focused on mineral alteration away from the intrusions, especially surrounding fractures.

Several tasks can be identified for implementation of the Paiute Ridge natural analogue:

- Characterize the geologic site, including stratigraphy and determination of the state of alteration of the host rocks before emplacement of the intrusive complex. Identify areas for detailed field studies.
- Map fracture-matrix alteration as a function of distance perpendicular to intrusive structures and determine changes in fracture and matrix porosity and permeability. Distances as far as 50 m or more from the intrusive body may be required.
- If possible, identify evaporation and condensate zones in the field. These zones will not have remained fixed in time, but will have advanced away from the intrusion with increasing time. Hence, it will not be possible to pinpoint an exact location.
- Perform modeling studies based on the observed hydrothermal alteration in the field and attempt to reproduce the observed alteration surrounding the intrusion. By calibrating the model at one distance, it may be possible to reproduce alteration observed at other distances. More likely, it may be possible to reproduce the general extent or trend of alteration at different distances from the intrusion.

5 CRITIQUE OF MATYSKIELA (1997)

In a recent paper, Matyskiela (1997) proposed the Paiute Ridge intrusive complex as a natural analogue for the Yucca Mountain repository. Matyskiela studied mineral alteration surrounding the 50-m-wide Papoose Lake sill located on the eastern edge of the Nevada Test Site. His analysis, however, was based on a pure heat conduction model that did not take into account the two-phase nature of the system. The pure conduction model indicated maximum temperatures in the tuff country rock of 550°C and cooling times ranging from a maximum of 400 years to only 10 years. The initial temperature of the sill used in his calculations was 1100°C. These results are in stark contrast to the much longer cooling times, on the order of several thousand years, calculated with the thermal and material parameters listed in Table 1. Matyskiela (1997) does not give the parameters used in his calculations. Most significant appears to be differences in thermal conductivity and porosity between the intrusion and tuff host rock that give rise to the higher temperatures. In the analytical solution used by Matyskiela (1997), different thermal and material properties are not possible, and the temperature at the intrusive-tuff interface is constrained to be half the initial intrusive temperature.

The major finding reported by Matyskiela (1997) is the alteration of glass shards to cristobalite and clinoptilolite within 60 m of the intrusion. He interpreted the alteration as hydrothermal in origin, resulting from emplacement of the intrusion. Most significant was the reported observation of complete filling of pore spaces at fracture-matrix interfaces,

thus creating open conduits for flow of infiltrating fluid along fractures. This observation, if true, could have potentially detrimental effects on the proposed Yucca Mountain repository.

Matyskiela (1997) presents evidence of mineral alteration in a photomicrograph (Matyskiela's Figure 3) of a fracture in the vicinity of a 50-m-wide intrusive sill emplaced in vitric tuff. The matrix adjacent to the fracture is altered to a narrow zone of clinoptilolite that partially grows into the fracture. Glass shards deeper in the matrix are completely or partially altered to clinoptilolite. Within the matrix, cristobalite was found replacing glass. Chalcedony forms a fracture filling; however, Matyskiela considers precipitation of chalcedony as being caused by infiltration, and unrelated to the thermal event. Matyskiela (1997) reports that mineral alteration surrounding fractures is not found at distances greater than 60 m from the sill, suggesting that infiltrating rainwater could not be responsible for the observed alteration. It is not clear, however, whether the alteration took place before emplacement of the sill or after, as assumed by Matyskiela (1997).

Matyskiela (1997) presents a simple single-component numerical model to explain the observations in the photomicrograph he shows. Diffusion of fracture pore water, supersaturated with cristobalite, into the vitric tuff matrix that is perpendicular to the fracture wall is considered to be the cause for formation of cristobalite. Liquid water in the fracture is presumed to be in equilibrium with amorphous silica, with concentrations ranging from 125 ppm to 350 ppm. Matyskiela (1997) interprets the evidence for hydrothermal alteration at Paiute Ridge—and, in particular, the cristobalite fracture-matrix sealing—as an indication that at the Yucca Mountain repository, movement of liquid water will occur in isolated conduits where it could move relatively unrestricted downward towards the repository horizon, with little or no imbibition into the rock matrix. Matyskiela (1997) estimates enhanced fracture flow to be as much as five times ambient conditions. This behavior is opposite to formation of a silica cap that has been predicted by recent simulations, in which fractures would become filled with quartz (or chalcedony) and further flow would be inhibited (Hardin, 1998). Thus a direct contradiction would appear to exist between modeling results and field observations purporting to represent an analogue of the repository environment.

There are a number of other problems with the analysis given by Matyskiela (1997). The time-temperature-saturation history of the intrusive system is not discussed. For this system to serve as a natural analogue for the repository, it must be demonstrated that boiling conditions persisted for at least several thousand years. No proof is offered that the alteration observed in the photomicrograph could not have formed prior to emplacement of the intrusion. The mathematical analysis given by Matyskiela (1997) appears to be incorrect, and it is not possible to reproduce his calculated porosity profile—although the presumably correct result is still consistent with porosity data he presents (see Appendix). Matyskiela (1997) states that alteration of the vitric tuff decreases away from the thermal source. While he presents no evidence of this, if true, such behavior would seem inconsistent with the predictions of a hydrothermal model. At the intrusion-tuff contact, where temperatures are the highest and are well above boiling, there should be minimal hydrothermal alteration simply because liquid water would not be present for long periods of time. Hydrothermal alter-

ation should, in fact, increase away from the intrusion, and reach maximum alteration at a distance where boiling conditions were sustained the longest, and then should decrease as the distance from the intrusion increases and approaches ambient conditions (see Figure 3).

6 CONCLUSION

Magmatic intrusions in tuffaceous rock above the water table offer a unique opportunity to study conditions analogous to the proposed Yucca Mountain high-level nuclear waste repository following emplacement of waste. The Paiute Ridge intrusive complex in partially saturated tuff appears to offer an ideal natural analogue site. Thermal conditions of sustained boiling at tens of meters from the intrusion for as long as several thousand years are similar to those of the proposed repository. The extent of hydrothermal alteration of the tuff caused by emplacement of the intrusive complex is, at present uncertain, and more field work is needed to clarify the situation. The outcome of additional field work could either indicate that very little alteration will be caused by heat released from the repository or that more extensive alteration should be expected, which could impact the overall performance of the repository.

From the preliminary analysis presented in this white paper several conclusions can be drawn:

- Preliminary field work indicates that the tuff stratigraphy must be better understood to evaluate pre- and post-intrusive alteration effects.
- Very little data is currently available to support THC-coupled process models of the thermal evolution of the repository. As a consequence, contradictory results have been obtained regarding the thermal effects of the repository on the tuff host rock.

7 ACKNOWLEDGEMENTS

The authors would like to thank Giday WoldeGabriel for helpful discussions and for pointing out the existence of the opal alteration zone located at a basaltic sill contact. In addition, we would like to thank Greg Valentine and Bruce Robinson for reviewing the manuscript.

8 REFERENCES

Broxton, D.E., D.L. Bish, and R.G. Warren, 1987, "Distribution and Chemistry of Diagenetic Minerals at Yucca Mountain, Nye County, Nevada," *Clays and Clay Minerals* **35** (2), 89–110.

Byers, F.M., Jr., and H. Barnes, 1967, *Geologic Map of the Paiute Ridge Quadrangle, Nye and Lincoln Counties, Nevada*, U.S. Geological Survey Map xx-xxx.

Carey, J.W., D.L. Bish, S.J. Chipera, and S.S. Levy, 1997, "Integrated Conceptual Model for Mineral Evolution," Los Alamos Yucca Mountain Project Milestone Report #SP321EM4.

Carter Krogh, K.E., and G.A. Valentine, 1996, "Structural Control on Basaltic Dike and Sill Emplacement, Paiute Ridge Mafic Intrusion Complex, Southern Nevada," Los Alamos National Laboratory report LA-13147-MS.

Crowe, B., S. Self, D. Vaniman, R. Amos, and F. Perry, 1983, "Aspects of Potential Magmatic Disruption of a High-Level Radioactive Waste Repository in Southern Nevada," *Journal of Geology* **91**, 259–276.

Drury, M.J., 1987, "Thermal Diffusivity of Some Crystalline Rocks," *Geothermics* **16**, 105–115.

Francis, N.D, 1997, "The Base-Case Thermal Properties for TSPA-VA Modeling," Sandia National Laboratories technical memorandum (April 16, 1997).

Geissman, J.W., 1998, University of New Mexico, personal communication.

Goff, F., 1995, "Paiute Ridge-Slanted Buttes, Half Pint Range, Nevada," Geologic map, Los Alamos National Laboratory technical memorandum (September 8, 1995).

Hardin, E., 1998, "Near-Field/Altered Zone Models Report," Lawrence Livermore National Laboratory report UCRL-ID-129179.

Keating, G.N., and J.W. Geissman, 1998, "Cooling History of Shallow-Level Intrusions and Host Tuffs, Paiute Ridge, Nevada: Field, Paleomagnetic, and Thermal Modeling Results," GSA Abstracts with Programs, **30**, October 1993, Toronto, Ontario, p. 107.

Keating, G.N., G.A. Zyvoloski, and G.A. Valentine, 1998, "Multiphase Thermal Modeling of Cooling Ignimbrites," *EOS: Trans. Am. Geophys. Union* **79** (45), F281.

Lichtner, P.C., 1999a, *FLOTRAN User's Manual*, Version 1.0, Los Alamos National Laboratory document.

Lichtner, P.C., 1999b, "Multicomponent Reactive Transport in Fractured Porous Media: Methods and Applications," to be published in *Dynamics of Fluids in Fractured Rocks: Concepts and Recent Advances* (International Symposium in Honor of Paul A. Witherspoon, Berkeley, CA, 1999).

Lichtner, P.C., and M.S. Seth, 1996, "Multiphase-Multicomponent Nonisothermal Reactive Transport in Partially Saturated Porous Media: Application to the Proposed Yucca Mountain HLW Repository," in Proceedings of the International Conference on Deep Geologic Disposal of Radioactive Waste, Canadian Nuclear Society, September 16–19 (1996), Winnipeg, Manitoba, Canada, pp. 3-133–3-142.

Matyskiela, W., 1997, "Silica Redistribution and Hydrologic Changes in Heated Fractured Tuff," *Geology* **25** (12), 1115-1118.

Minor, S.A., 1995, "Superposed Local and Regional Paleostresses: Fault-Slip Analysis of Neogene Extensional Faulting Near Coeval Caldera Complexes, Yucca Flat, Nevada," *Journal of Geophysical Research* **100**, 10,507–10,528.

Nitao, J., 1998, "Thermohydrochemical Alteration of Flow Pathways Above and Below the Repository," in Chapter 5.6 of "Near-Field/Altered Zone Models Report," E. Hardin, Ed., Lawrence Livermore National Laboratory report UCRL-ID-129179.

Peters, R.R., E.A. Klavetter, I.J. Hall, S.C. Blair, P.R. Heller, and G.W. Gee, 1984, "Fracture and Matrix Hydrologic Characteristics of Tuffaceous Materials from Yucca Mountain, Nye County, Nevada," Sandia National Laboratory report SAND84-1471.

Ratcliff, C.D., J.W. Geissman, F.V. Perry, B.M. Crow, and P.K. Zeitler, 1994, "Paleomagnetic Record of a Geomagnetic-Field Reversal from Late Miocene Mafic Intrusions, Southern Nevada," *Science* **266**, 412–416.

Robinson, B.A., A.V. Wolfsberg, H.S. Viswanathan, G.Y. Bussod, C.W. Gable, and A. Meijer, 1997, "The Site-Scale Unsaturated Zone Transport Model of Yucca Mountain, Milestone SP25BM3," Los Alamos National Laboratory document.

Sawyer, D.A., R.J. Fleck, M.A. Lanphere, R.G. Warren, D.E. Broxton, and M. R. Hudson, 1994, "Episodic Caldera Volcanism in the Miocene Southwestern Nevada Volcanic Field: Revised Stratigraphic Framework, 40Ar/39Ar Geochronology, and Implications for Magmatism and Extension," *Geological Society of America Bulletin* **106**, 1304–1318.

Valentine, G.A., G. WoldeGabriel, N.D. Rosenberg, K.E. Carter Krogh, B.M. Crowe, P. Stauffer, L.H. Auer, C.W. Gable, F. Goff, R. Warren, and F.V. Perry, 1998, "Physical Processes of Magmatism and Effects on the Potential Repository: Synthesis of Technical Work Through Fiscal Year 1995, in, Perry, F.V., B.M. Crowe, G.A. Valentine, and L.M. Bowker, eds., Volcanism studies: final report for the Yucca Mountain Project, Los Alamos National Laboratory Report LA-13478, 554 p.

Warren, R.G., 1995, "Results of Field work with Giday, Fraser, and Karen," Los Alamos National Laboratory technical memorandum (August, 25).

Whitbeck, M., and W.E. Glassley, 1998, "Reaction-Path Model for Water Chemistry and Mineral Evolution in the Altered Zone," in Chapter 5.4 of "Near-Field/Altered Zone

Models Report," E. Hardin, Ed., Lawrence Livermore National Laboratory report UCRL-ID-129179.

Wu, Y.S., A.C. Ritcey, C.F. Ahlers, A.K. Mishra, J.J. Hinds, and G.S. Bodvarsson, 1997, "Providing Base-Case Flow Fields for TSPA-VA: Evaluation of Uncertainty of Present-Day Infiltration Rates Using DKM/Base-Case and DKM/Weeps Parameters Sets," Lawrence Berkeley National Laboratory Level 4 Milestone report SLX01LB2.

Zyvoloski, G.A., B.A., Robinson, Z.V., Dash, and L.L., Trease, 1997, "Summary of the Models and Methods for the FEHM Application—A Finite-Element Heat- and Mass-Transfer Code, Los Alamos National Laboratory report LA-13307-MS.

APPENDIX: ANALYSIS OF MATYSKIELA'S (1997) DIFFUSION MODEL

In a recent paper, Matyskiela (1997) suggested as a natural analogue for the proposed Yucca Mountain high-level nuclear waste repository the Papoose Lake sill that intruded into a tuffaceous host rock above the water table. Matyskiela (1997) argued that as a result of heat evolving from the intrusion and remobilization of liquid water, cristobalite precipitated within the rock matrix along fractures, thereby sealing fractures from the matrix and creating fast pathways to enhance infiltration.

A.1 Model Formulation

The conceptual model posed by Matyskiela (1997) involves a single-component system to describe mineral alteration in which fracture pore water diffusives into the tuff matrix. The fracture pore water is assumed to have come to equilibrium with respect to amorphous silica or cristobalite at 95°C with concentrations varying between 115 ppm and 350 ppm. The matrix is presumed to be in equilibrium with respect to cristobalite at 115 ppm. Silica polymorphs, quartz and chalcedony, are not allowed to precipitate. As solute diffuses from the fracture into the rock matrix, cristobalite precipitates under supersaturated conditions.

For the chemical reaction

$$\mathcal{A} \rightleftharpoons \mathcal{A}_{(s)}, \tag{A.1}$$

involving a single solute species $\mathcal{A}$ and solid $\mathcal{A}_{(s)}$ with reaction rate I_s, the transient mass transport equation for diffusion and reaction of the solute species with concentration $C(x, t)$ has the form

$$\frac{\partial}{\partial t}(\phi C) - \frac{\partial}{\partial x}\left(\tau\phi D\frac{\partial C}{\partial x}\right) = -I_s. \tag{A.2}$$

The solute concentration evolves with time t, with diffusion taking place along the x-axis perpendicular to the fracture. The diffusivity, porosity, and tortuosity factor of the matrix are denoted by D, ϕ, and τ, respectively. Mass transfer of the solid phase is described by the equation

$$\frac{\partial \phi_s}{\partial t} = \overline{V}_s I_s, \tag{A.3}$$

where the solid concentration is represented by the volume fraction ϕ_s, and $\overline{V}_s$ denotes the solid molar volume.

For the reaction as written in Eq. (A.1), the reaction rate I_s can be expressed in a

number of alternative forms as

$$I_s = s(k_f C - k_b), \tag{A.4}$$
$$= -k_b s(1 - KC), \tag{A.5}$$
$$= k_f s(C - C_{\text{eq}}). \tag{A.6}$$

The quantities k_f and k_b denote the forward and backward kinetic rate constants which are related to the equilibrium constant K for the reaction by

$$K = \frac{k_f}{k_b}. \tag{A.7}$$

The equilibrium concentration C_{eq} is related to the equilibrium constant by

$$C_{\text{eq}} = K^{-1}. \tag{A.8}$$

The rate is proportional to the mineral surface area s, in general, a function of the solid concentration ϕ_s. Porosity and solid volume fraction are related by the expression

$$\phi = 1 - \phi_s, \tag{A.9}$$

valid for the situation in which the rock matrix consists of a single mineral, and assuming that the total porosity can be identified with the connected porosity that takes part in diffusive mass transport.

A characteristic feature of the reactive-transport equations is that for mineral precipitation/dissolution reactions, the solute concentration rapidly reaches a stationary state compared to the time required for significant changes to occur in the solid concentration and, hence, changes in the porosity of the porous medium (Lichtner, 1988). The stationary-state solution is obtained by solving the ordinary differential equation

$$\tau\phi D\frac{d^2C}{dx^2} = I_s, \tag{A.10}$$

in which porosity and the tortuosity factor are considered constants. The solution to Eq. (A.10), with appropriate boundary conditions, has the general form

$$C = C_1 e^{qx} + C_2 e^{-qx} + C_{\text{eq}}, \tag{A.11}$$

where the quantity q is defined as

$$q = \sqrt{\frac{k_f s}{\tau\phi D}}. \tag{A.12}$$

The coefficients C_1 and C_2 are determined through boundary conditions imposed on the system at the fracture-matrix interface and within the matrix. The quantity q may be interpreted as the inverse of the equilibration length for the reaction—that is, the characteristic length scale over which the solute concentration reaches equilibrium with respect to the solid.

Several boundary conditions are possible within the tuff matrix. Two possibilities are to consider a system of finite length L with either a fixed concentration or a zero-flux boundary condition at a distance L from the fracture. Another possibility is to consider an infinite length system with zero flux at an infinite distance from the fracture. All three approaches give similar results for the conditions of the problem. In the following subsections, the stationary-state solute transport equation is solved for both finite and infinite length systems. For a finite length system, concentration and zero-flux boundary conditions are compared.

A.1.1 Infinite Length System

For an infinite length system, the stationary-state solution can be expressed in the form

$$C(x) = C_{eq} + \Delta C_0 e^{-qx}, \tag{A.13}$$

where

$$\Delta C_0 = C_0 - C_{eq}, \tag{A.14}$$

and C_0 denotes the solute concentration at the fracture-matrix interface. Note that $\Delta C_0 > 0$ for precipitation to occur, because in that case $C_0 > C_{eq}$. The change in solid concentration with time and distance is obtained by integrating Eq. (A.3), assuming the rate I_s is constant, determined from the stationary-state aqueous concentration, to give

$$\phi_s(x, t) = \phi_s^0 + \overline{V}_s k_f s t \Delta C_0 e^{-qx}, \tag{A.15}$$

where ϕ_s^0 denotes the initial solid volume fraction. For fixed time, the solid concentration decreases exponentially with distance from the fracture. From this result, the porosity profile can be expressed as a function of time and space as

$$\phi(x, t) = \phi_0 - t k_f s \overline{V}_s \Delta C_0 e^{-qx}, \tag{A.16}$$

with initial porosity ϕ_0.

The time t_0 required for the solid to completely occupy all available pore space at the fracture-matrix contact follows from the equation

$$\phi(x = 0, t_0) = 0, \tag{A.17}$$

yielding

$$t_0 = \frac{\phi_0}{k_f s \overline{V}_s \Delta C_0}. \tag{A.18}$$

Using this result, the porosity at any time $t \leq t_0$ can be written as

$$\phi(x, t_0) = \phi_0 \left[1 - \frac{t}{t_0} e^{-qx}\right]. \tag{A.19}$$

In obtaining this relation it is assumed that the solid surface area is constant. The case of variable surface area is considered in subsection A.2.

A.1.2 Finite Length System

Two boundary conditions are considered for a finite length system corresponding to constant concentration and zero flux.

A.1.2.1 Concentration Boundary Condition

For a system with finite length L and concentration boundary conditions of the form

$$C(0) = C_0, \tag{A.20}$$

and

$$C(L) = C_{\text{eq}}, \tag{A.21}$$

it follows that

$$C_1 = \frac{\Delta C_0}{1 - \mathrm{e}^{2qL}}, \tag{A.22}$$

and

$$C_2 = -\frac{\Delta C_0 \mathrm{e}^{2qL}}{1 - \mathrm{e}^{2qL}}. \tag{A.23}$$

This yields the explicit solution for the solute concentration

$$C(x) = \frac{\Delta C_0 \mathrm{e}^{qL}}{1 - \mathrm{e}^{2qL}} \left\{ \mathrm{e}^{q(x-L)} - \mathrm{e}^{-q(x-L)} \right\} + C_{\text{eq}}. \tag{A.24}$$

The time it takes for the solid to completely occupy all available pore space at the fracture-matrix contact is the same as that for an infinite system, regardless of the value for qL, given by t_0 defined in Eq. (A.18). The porosity can be expressed as

$$\phi(x, t) = \phi_0 \left[1 - \frac{t}{t_0} \frac{\mathrm{e}^{qL}}{1 - \mathrm{e}^{2qL}} \left\{ \mathrm{e}^{q(x-L)} - \mathrm{e}^{-q(x-L)} \right\} \right]. \tag{A.25}$$

It follows that in the limit $qL \gg 1$,

$$\phi(x, t_0) \longrightarrow \phi_0 \left[1 - \frac{t}{t_0} \mathrm{e}^{-qx} \right], \quad (qL \gg 1). \tag{A.26}$$

Thus, if the dimensionless quantity qL is sufficiently large, or equivalently, if the equilibration length is much smaller than the length of the system, the results for a finite length system become identical to those of an infinite system.

A.1.2.2 Zero-Flux Boundary Condition

For the zero-flux boundary condition imposed at $x = L$ given by

$$\left(\frac{\partial C}{\partial x}\right)_{x=L} = 0, \tag{A.27}$$

the coefficients C_1 and C_2 become

$$C_1 = \frac{\Delta C_0}{1 + e^{2qL}}, \tag{A.28}$$

and

$$C_2 = \frac{\Delta C_0 e^{2qL}}{1 + e^{2qL}}. \tag{A.29}$$

The stationary-state solute concentration is given by

$$C(x) = \frac{\Delta C_0 e^{qL}}{1 + e^{2qL}} \left\{e^{q(x-L)} + e^{-q(x-L)}\right\} + C_{eq}. \tag{A.30}$$

From this result the expression for the porosity becomes

$$\phi(x, t) = \phi_0 \left[1 - \frac{t}{t_0} \frac{e^{qL}}{1 + e^{2qL}} \left\{e^{q(x-L)} + e^{-q(x-L)}\right\}\right]. \tag{A.31}$$

It follows that in the limit $qL \gg 1$,

$$\phi(x, t_0) \longrightarrow \phi_0 \left[1 - \frac{t}{t_0} e^{-qx}\right], \quad (qL \gg 1), \tag{A.32}$$

which is identical to the fixed concentration boundary condition case.

A.2 Variable Surface Area

If the surface area depends on porosity, for example, in the form of a power law

$$s = s_0 \left(\frac{\phi}{\phi_0}\right)^n, \tag{A.33}$$

for some constant n, then using $\phi_s = \phi_0 - \phi$, the change in porosity becomes for an infinite length system

$$\frac{\partial \phi}{\partial t} = -\overline{V}_s k s_0 \left(\frac{\phi}{\phi_0}\right)^n \Delta C_0 e^{-qx}. \tag{A.34}$$

The time for the porosity to become zero is related to t_0 by

$$t_0' = \frac{t_0}{1 - n}. \tag{A.35}$$

For $n = 2/3$, $1 - n = 1/3$, and the time for the porosity to go to zero take three times longer compared to constant surface area.

A.3 Fit to Observed Porosity Profile

A fit to the observed porosity profile presented by Matyskiela (1997) can be obtained by varying the inverse equilibration length q. Values for the fracture concentration C_0 range between the equilibrium values for cristobalite and amorphous silica. Cristobalite is assumed to be the precipitating silica polymorph. Because the matrix fluid is assumed to be in equilibrium with respect to cristobalite, precipitation can occur only for fracture solutions which are supersaturated with respect to cristobalite. Values for various parameters used in the fit are listed in Table 2. Once a value for q is obtained, the surface area of the solid phase can be determined by inverting Eq. (A.12) to yield the result

$$s = q^2 \frac{\tau \phi_0 D}{k_f}. \tag{A.36}$$

However, it should be kept in mind that the surface area may not remain constant and may very likely increase as precipitation proceeds.

Table 2: Silica Precipitation Modeling Parameters (Rimstidt and Barnes, 1980)

Property	Value	Comment
ϕ_0	0.2	
k_f	$10^{-7.77}$	all silica polymorphs
k_b	$10^{-10.48}$	cristobalite
D_{eff}	3×10^{-9} cm^2/s	$(\tau \phi D)$
L	5 cm	
C_0	350 ppm	amorphous silica
	125 ppm	cristobalite
C_{eq}	113.75 ppm	calculated
$\overline{V}_s$	25.74 cm^3 mole^{-1}	chalcedony

Porosity is plotted in Figure 11 as a function of distance corresponding to the time for complete sealing at the fracture-matrix interface. Zero-flux and fixed concentration boundary conditions for a finite system are contrasted with an infinite system. The steeper curve fits better with Figure 5 in Matyskiela (1997). However, both sets of curves appear consistent with the data presented by Matyskiela (1997) in his Figure 5.

Several remarks can be made regarding the analysis given by Matyskiela (1997).

- Other explanations may be possible for the observed alteration of glass to clinoptilolite and cristobalite. Conclusive proof is not given whether the alteration pre- or post-dated the sill intrusion. Reaction of fines and dust with high specific surface area could also be responsible for the alteration.

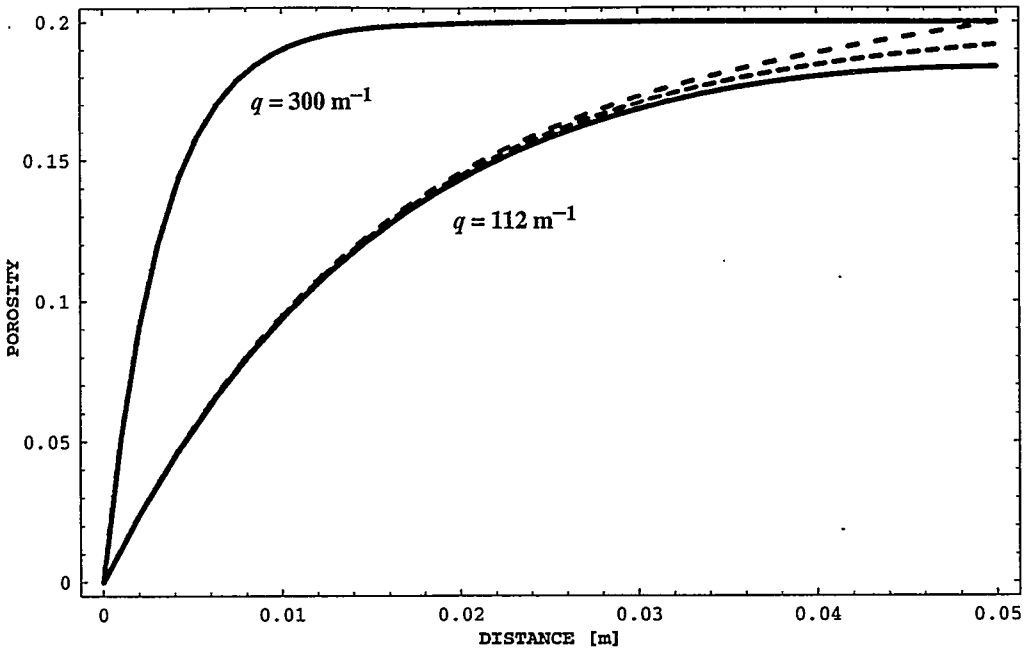

Figure 11: Porosity profile into the rock matrix for $q = 300\ \mathrm{m}^{-1}$ (upper curves) and $q = 112\ \mathrm{m}^{-1}$ (lower curves). Red corresponds to a zero-flux boundary condition, blue to a fixed concentration boundary condition, and green to an infinite system. All three curves coincide for $q = 300\ \mathrm{m}^{-1}$.

- Inconsistent boundary conditions are given as *both* concentration and zero flux at a distance L from the fracture wall, which over-determines the problem.

- The definition of coefficient α appearing in Matyskiela's Eq. (2) appears to be incorrectly given as $\alpha = \Delta C_0/(1 - \exp(\lambda L))^2$. According to the results given above, $\alpha = \Delta C_0/(1 + \exp(2\lambda L))$.

- Matyskiela (1997) states that fracture silica concentrations above 125 ppm generate approximately the same sealed fracture-margin porosity profile, but over varying times. He states that 350 ppm silica requires 5 years, and 125 ppm silica requires 105 years. The time it takes to seal the fracture-margin porosity is inversely proportional to ΔC_0. The ratio of times is given by

$$\frac{(t_0)_{125ppm}}{(t_0)_{350ppm}} = \frac{C_0^{350\mathrm{ppm}} - C_{\mathrm{eq}}}{C_0^{125\mathrm{ppm}} - C_{\mathrm{eq}}} \simeq 21. \tag{A.37}$$

  This implies the following value for C_{eq}:

$$C_{\mathrm{eq}} = \frac{21 C_0^{125\mathrm{ppm}} - C_0^{350\mathrm{ppm}}}{20} \simeq 113.75\mathrm{ppm}, \tag{A.38}$$

  which is slightly undersaturated with respect to cristobalite(α), having an equilibrium concentration of 115.459 ppm at 95°C.

- The absolute sealing time according to Eq. (A.18) depends on the surface area s, which may be related to q through Eq. (A.36). Thus, the absolute sealing time can be

expressed as [taking $n = 2/3$ in Eq. (A.33)]

$$t_0 = \frac{3}{\overline{V}_s \tau D q^2 \Delta C_0}, \quad (A.39)$$

which varies inversely with q^2, or, solving for q,

$$q = \sqrt{\frac{3}{\overline{V}_s \tau D t_0 \Delta C_0}}. \quad (A.40)$$

With the values given in Table 2, $q \simeq 112$. This value for q, however, does not give a precipitation front as sharp as that obtained by Matyskiela (see Figure 11). It would also imply much shorter precipitation times than those reported by Matyskiela. Both values, however, appear consistent with the data presented in Figure 5 of Matyskiela (1997).

- Matyskiela (1997) does not state the mineral surface area (or pore diameter) he used in the calculation, which is presumably held constant. From Eq. (A.36), a value of 723.57 cm^{-1} is obtained, corresponding to a grain size of $b = 0.0829$ mm ($s = 6/b$).

A.4 References

Lichtner, P.C., 1988, "The Quasi-Stationary State Approximation to Coupled Mass Transport and Fluid-Rock Interaction in a Porous Medium," *Geochimica et Cosmochimica Acta* **52**, 143–165.

Matyskiela, W., 1997, "Silica Redistribution and Hydrologic Changes in Heated Fractured Tuff," *Geology* **25** (12), 1115–1118.

Rimstidt, J.D., and H.L. Barnes, 1980, "The Kinetics of Silica-Water Reactions," *Geochimica et Cosmochimica Acta* **44**, 1683–1699.